

Where are the missing Kuiper Belt binaries?

Wladimir Lyra^{a,*}

^aNew Mexico State University, Department of Astronomy, PO Box 30001 MSC 4500, Las Cruces, 88001, NM, USA

ARTICLE INFO

Keywords:
 Kuiper belt
 Planetesimals
 Binaries
 Origin, solar system
 Planetary formation

ABSTRACT

In this letter, we call attention to a gap in binaries in the Kuiper belt in the mass range between $\approx 10^{19}$ – 10^{20} kg, with a corresponding dearth in binaries between 4th and 5th absolute magnitude H . The low-mass end of the gap is consistent with the truncation of the cold classical population at 400 km, as suggested by the OSSOS survey, and predicted by simulations of planetesimal formation by streaming instability. The distribution of magnitudes for all KBOs is continuous, which means that many objects exist in the gap, but the binaries in this range have either been disrupted, or the companions are too close to the primary and/or too dim to be detected with the current generation of observational instruments. At the high-mass side of the gap, the objects have small satellites at small separations, and we find a trend that as mass decreases, the ratio of primary radius to secondary semimajor increases. If this trend continues into the gap, non-Keplerian effects should make mass determination more challenging.

1. Introduction

The Kuiper belt is a region of the solar system populated by small bodies, remnants from the planet formation process. Following the discovery of Pluto (Slipher, 1930; Tombaugh, 1946) and Charon (Christy and Harrington, 1978), the belt now comprises thousands of objects (c.f. Barucci et al., 2008; Prialnik et al., 2020) discovered after 1992 (Jewitt and Luu, 1993). With the comprehensive statistics, a picture has emerged that the current Kuiper belt is a remnant of a much more massive primordial belt of objects, that has been sculpted by the evolution of the orbits of the giant planets (Stern, 1996; Morbidelli and Valsecchi, 1997; Stern and Colwell, 1997; Morbidelli et al., 2003; Hahn, 2003; Tsiganis et al., 2005; Gomes et al., 2005; Morbidelli et al., 2008; Batygin et al., 2011; Dones et al., 2015; Malhotra, 2019; Morbidelli and Nesvorný, 2020; Bottke et al., 2023). The objects are classified according to their interaction with Neptune: Plutinos are objects in the 3:2 resonance with Neptune; the Scattered Disk comprises objects whose perihelia approaches Neptune (30–35 AU), having thus wide eccentricity and inclination ranges; the Classical KBOs have moderately low eccentricity, and orbit between 42 and 48 AU, relatively undisturbed by Neptune. This class is subdivided into a dynamically hot and a dynamically cold population (Bernstein et al., 2004; Noll et al., 2008b; Fraser et al., 2010; Petit et al., 2011), with the cold classics probably forming in situ (Parker and Kavelaars, 2010; Batygin et al., 2011) thus representing the only population of pristine planetesimals in the Solar System. Conversely, the larger KBOs were probably formed inside 25 AU as theoretical mechanisms for planetary growth (planetesimal and pebble accretion) cease to yield sufficient mass accretion rates to form them beyond this distance (Johansen et al., 2015; Lyra et al., 2023; Cañas et al., 2024).

In contrast to the asteroid belt between Mars and Jupiter, Kuiper belt objects show a much higher proportion of binaries (Noll et al., 2008a), which is expected from their much larger Hill radii for the same mass. The presence of a companion enables the determination of dynamical masses (if an orbit can be fit) and, through stellar occultation observations (Sicardy et al., 2006; Braga-Ribas et al., 2013; Brown, 2013a) or, less accurately, thermal radiometry (Stansberry et al., 2008; Müller et al., 2010; Brown and Butler, 2017), volume measurements can be made; together, these allow for determining density. The resulting density vs radius correlation (Brown, 2013b; Grundy et al., 2015; McKinnon et al., 2017) or equivalently density vs mass (Noll et al., 2020; Cañas et al., 2024) reveals a trend in which smaller objects tend to be lower density, whereas the larger objects tend to be higher density, which is interpreted as a result of porosity removal (Bierson and Nimmo, 2019; Noll et al., 2020) and/or fundamental differences in composition (Brown, 2013b; Cañas et al., 2024). While much effort has been devoted to explaining the density trend, a major feature of this plot has received less attention: a gap over a decade in mass with a dearth of binaries.

In this letter, we are interested in the question: is this mass gap real (i.e., few binaries in this range exist), or is it a result of observational bias (i.e., the binaries exist but remain undiscovered). We interpret it as a missing binaries problem, and advance a few possible explanations for its existence.

2. The mass gap

The gap is illustrated in Fig. 1, between roughly 10^{19} – 10^{20} kg, containing only two objects (2002 WC₁₉ and Huya), whereas many objects are present in higher and lower masses. The gap is also visible in Fig. 3 of Brown (2013b), Fig. 5 of Grundy et al. (2015), Fig. 1 of McKinnon et al. (2017), Fig. 1 of Bierson and Nimmo (2019), and Fig. 1 of Rommel et al. (2025), in radius, ranging between ≈ 200 –350 km. Plotting in mass as in the Fig. 5 of Noll et al. (2020) and Fig. 1 of Cañas et al. (2024) makes the gap

*Corresponding author

 wlyra@nmsu.edu (W. Lyra)

 <http://astronomy.nmsu.edu/wlyra/> (W. Lyra)

ORCID(s): 0000-0002-3768-7542 (W. Lyra)

Kuiper belt mass gap

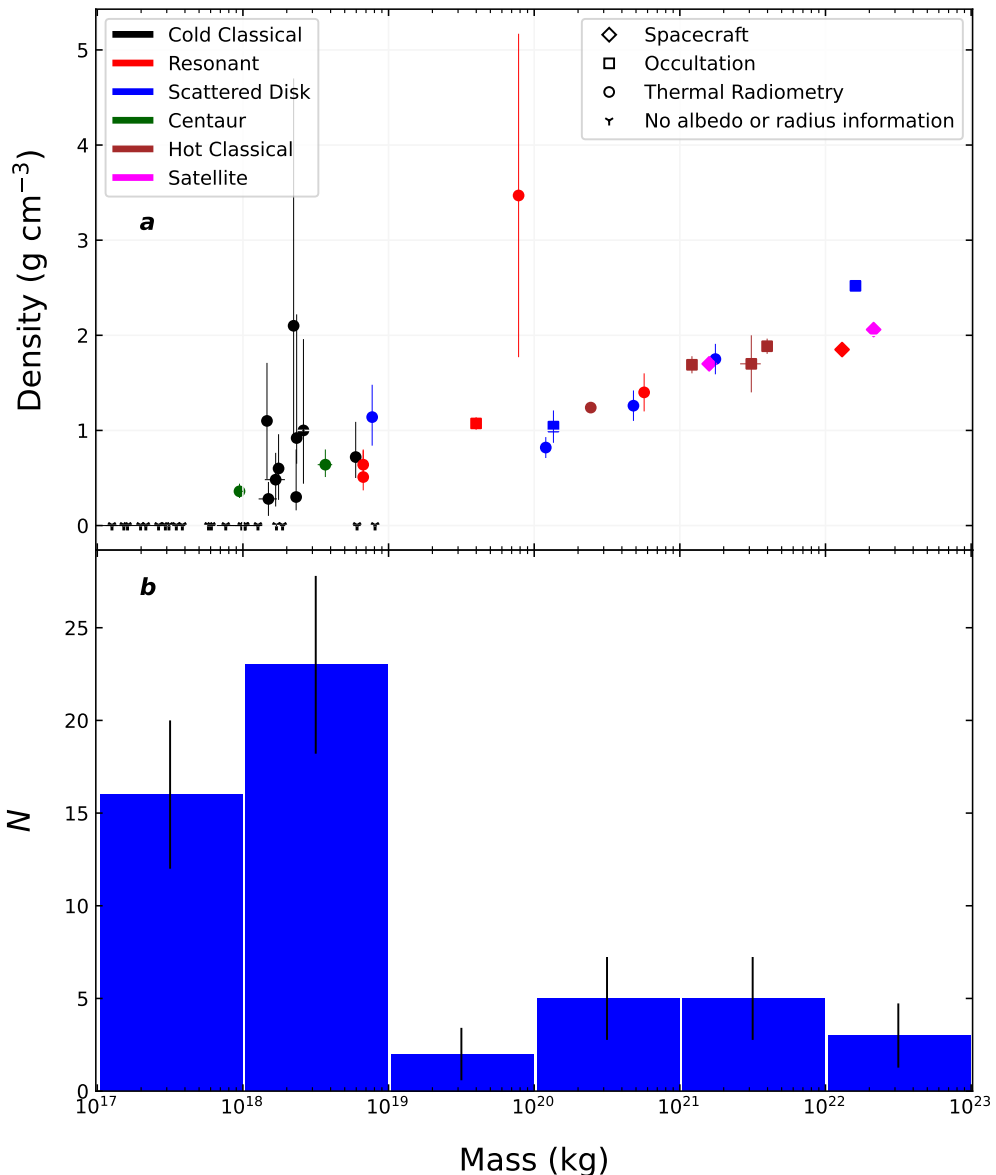


Figure 1: a): The currently known mass vs. density distribution of Kuiper Belt objects, showing a dearth of objects in the mass range between $\approx 10^{19} - 10^{20}$ kg. Different symbols mark the method used for radius determination, and the colors code the population the object belongs to. Objects with no radius information are plotted at zero density. The two objects in the gap are Huya and 2002 WC₁₉; both objects are of higher density than the suggested density trend at their masses. b): Mass histogram of the same objects as above.

more prominent by cubing the range, to about a decade. The data we use is from Johnston (2019, hereafter J19), with masses from non-Keplerian orbital fits from (Proudfoot et al., 2024) when available. We also use updated data for the following objects: for Quaoar we use recent occultation data (Morgado et al., 2023; Pereira et al., 2023); for Gonggong we use the radius and density data from Kiss et al. (2019); for Pluto and Charon we use New Horizon's updated data from Brozović and Jacobson (2024); for Huya we use the recent occultation data from Rommel et al. (2025); for Borasisi we use asymmetric error bars for density ($^{+2.6}_{-1.2} \text{ g cm}^{-3}$) from Vilenius et al. (2014, hereafter V14); for 2002 WC₁₉ we used the density determination $3.47 \pm 1.7 \text{ g cm}^{-3}$ from Kovalenko

et al. (2017) using the thermal radiometry radius from Lellouch et al. (2013). We remove the following objects: Mors, because the density of 0.75 g cm^{-3} listed in J19 is the assumed, not measured, density in Sheppard et al. (2012); 2001 QW₃₂₂, because the reference for density (Petit et al., 2008) assumes an albedo to find a radius and thus density measurement; 2001 QG₂₉₈, as this system is a contact binary, according to Lacerda (2011). The albedo for this object is derived from infrared observations, and a shape model is used to derive a density from the light curves (Descamps, 2015). The mass is not dynamical, but model-dependent. Finally, we add the following objects: 2003 QA₉₁, although the object has no density listed in J19, it has dynamical

mass, from Grundy et al. (2019, hereafter G19), radius from thermal radiometry from V14 and primary-to-secondary radius ratio from Noll et al. (2008a). With this information, we could calculate a density of $0.48 \pm 0.28 \text{ g cm}^{-3}$; 2002 VT₁₃₀, for which we could similarly calculate a density of $0.28 \pm 0.18 \text{ g cm}^{-3}$. The masses used are the mass of the primary, derived using the system mass combined with primary to secondary radius ratio considering equal density, a safe assumption for the cold classicals. Equal density is not a good assumption for the higher-mass objects, but in that case the satellite contributes a small fraction of the system mass, and the equal density assumption will not significantly affect the results (we verified that our conclusions are unchanged if using system mass, see Appendix A). For Triton, Pluto, and Charon we use their individually determined masses.

Fig. 1a shows a density vs mass plot of the binaries with dynamical mass determination down to 10^{17} kg ; the method used for radius determination is shown with different symbols, and we color code the different populations. Objects with mass but no density information are plotted at zero density. Fig. 1b is a mass histogram of the same objects as Fig. 1a. In Fig. 2 we plot the distribution of absolute magnitudes H of the binaries (blue)¹, and the distribution of all KBOs (red), obtained from the JPL Small-Body Database². A dearth in binaries is seen between magnitudes 4 and 5, whereas the distribution of KBOs magnitudes is continuous.

3. Discussion

As noted by Bernstein et al. (2023), there is a population difference between the smallest and largest known binary KBOs, in that the former tend to have more widely separated, equal-sized binaries (making them easier to detect), whereas the latter tend to have small satellites on tighter orbits, suggesting different formation scenarios. Indeed, the difference is evident in the population breakdown show in Fig. 1a, in that cold classicals are all on the low-mass side of the gap. At the high-mass side of the gap, the objects are primarily scattered disk objects and hot classicals. The low-mass edge of the gap seems to be consistent with the cold classical mass distribution: the OSSOS survey (Kavelaars et al., 2021) finds that the distribution of cold classicals is complete to about 400 km diameter. At a density of 0.5 g cm^{-3} , this diameter corresponds to $\approx 1.68 \times 10^{19} \text{ kg}$, consistent with the beginning of the mass gap. We conclude that the low-mass end of the gap at 10^{19} kg is the high-mass end of the cold classical population, set by the dynamics of planetesimal formation.

The high-mass end of the gap at 10^{20} kg is less clear. At the high-mass side of the gap the objects are mostly hot classicals, scattered disk and resonant bodies. These objects have smaller satellites, of low mass ratio compared to the primaries. A few possibilities emerge.

¹Obtained from <http://www2.lowell.edu/users/grundy/ttns/status.html>

²https://ssd.jpl.nasa.gov/tools/sbdb_query.html

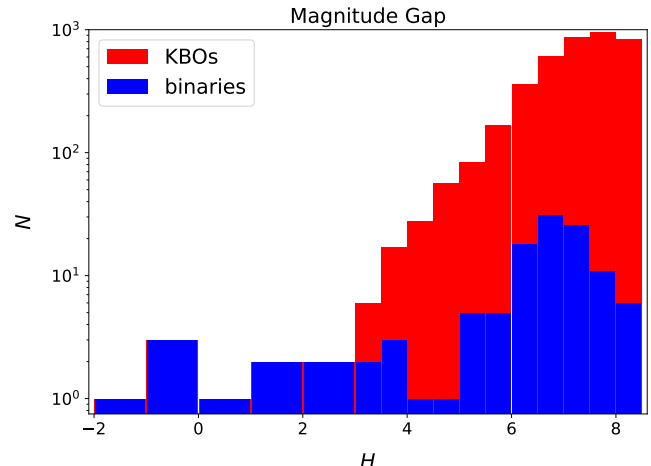


Figure 2: The gap is also present in the distribution of magnitudes, as a dearth of binaries between fourth and fifth magnitude (blue bins). Note that the distribution of KBOs is continuous in this magnitude range, showing that objects in this magnitude range (and thus mass range) exist. The two objects in the gap are Salacia ($H = 4.24 \pm 0.02$) and 2000 YW₁₃₄ ($H = 4.72 \pm 0.03$). The two objects in the mass gap (Huya and 2002 WC₁₉) are on the dim side of the magnitude gap.

If the binaries are actually missing, we could expect that the binary disruption was due to the interaction with Neptune, that implanted the objects in their current orbit in the Kuiper belt. Indeed, these objects should have formed inside 25 AU, as pebble accretion is not efficient beyond it (Lyra et al., 2023). These objects were implanted by Neptune into their current orbits over about 15 AU worth of migration. Given how some cold classicals binaries are weakly bound and easily disrupted, binaries have to be tightly bound to survive close encounters with Neptune (Parker and Kavelaars, 2010) or with the ensemble of planetesimals (Campbell et al., 2023, 2025).

In Fig. 3a we plot the semimajor axis of the binary as a fraction of the Hill radius R_H . The data is taken from J19, and the color and symbol scheme follows that of Fig. 1, except that now we split the objects with no density information into “assumed albedo” and “assumed density”. For the multiples, the semimajor axis of the innermost satellite was used: Charon for Pluto, Namaka for Haumea, and Hiisi for Lempo³. In addition to the error in a/R_H we add whiskers (thinner lines) to mark the eccentricity excursions, both of the orbit of the secondary and the binary orbit around the sun. The grey dotted line marks the 7% threshold usually quoted for ultra-wide binaries (Parker et al., 2011; Brunini and Zanardi, 2016). It is seen that the high-mass objects are all tight binaries, with a/R_H between 10^{-3} and 10^{-2} . This is at first counter-intuitive in light of the findings of Campbell et al. (2025), who show that the ultra-wide binaries started as relatively tighter binaries, and got their semi-major axes increased in the first 100 Myr of solar system history by

³The Lempo system actually has a third body, Paha, of diameter 132_{-19}^{+17} km. A hierarchical triple, their orbits deviate significantly from Keplerian.

Kuiper belt mass gap

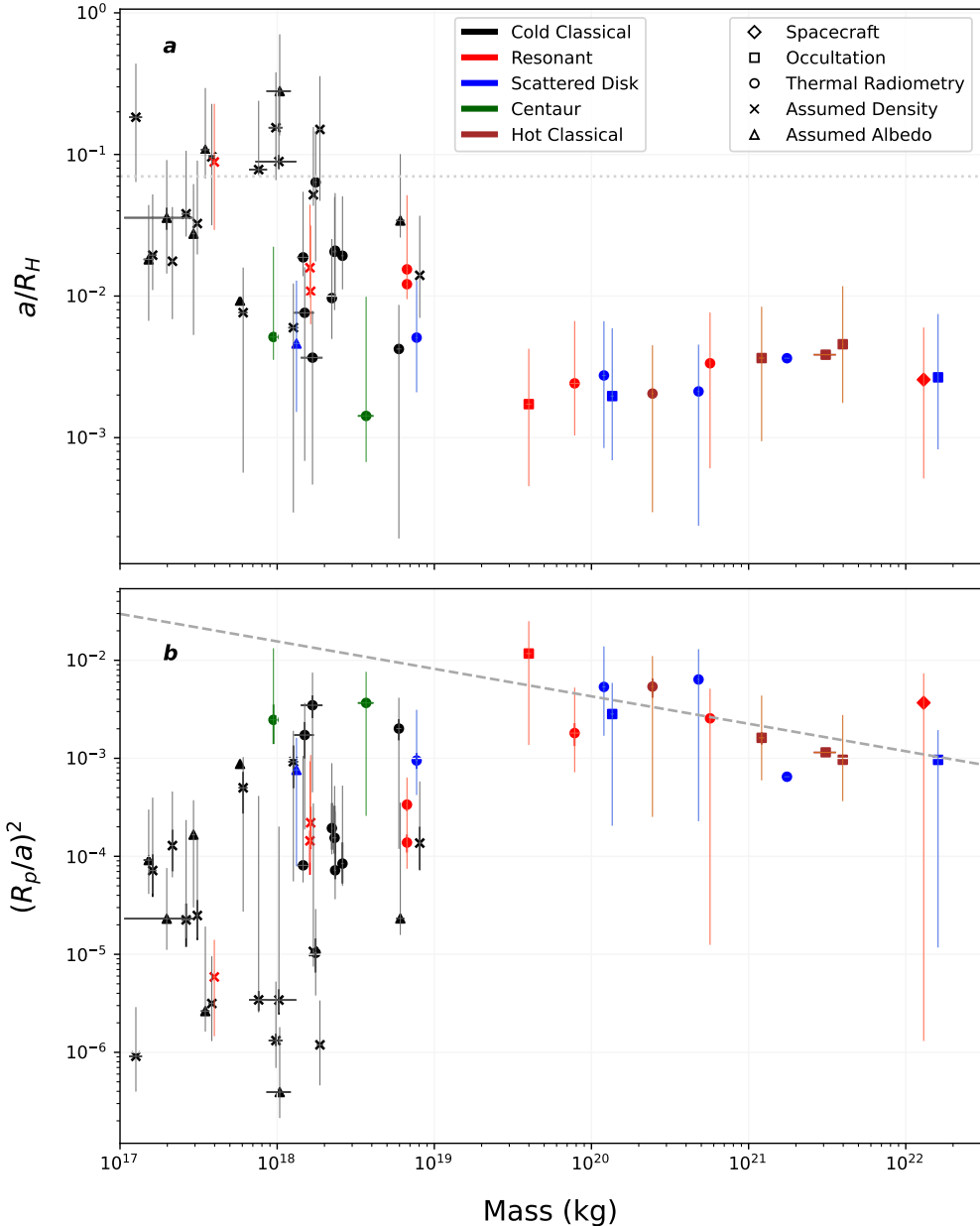


Figure 3: a): Semimajor axis of the secondary as a fraction of the binary Hill radius (a/R_H). The color code and symbols follow the same pattern as Fig. 1a, except we split the objects with no density information into those for which the radius estimate assumed density and those for which the radius estimate assumed albedo. Whiskers mark the range of eccentricity excursion. The higher mass objects are tight binaries with a flat distribution of a/R_H , whereas the low mass objects have wider separations. The horizontal dotted line at $a/R_H = 0.07$ marks the transition to ultra-wide binaries. Even though they are cold classicals, these ultra-wide binaries are not primordial, as they would be dissociated by encounters with other planetesimals scattered into the cold classical region (Campbell et al., 2025). That the high-mass objects lack a similar population of dynamically widened binaries suggests that, during their growth, they might have lost their primordial satellites. b): Plotting $(R_p/a)^2$ where R_p is the radius of the primary and a is the semi-major axis of the secondary, shows decreasing trend with mass for the objects in the high-mass side of the mass gap, while no trend is seen for the low-mass population. The dashed line is the linear regression of high-mass objects. If binaries in the gap follow the same trend, non-Keplerian effects on the orbit should be significant. Huya and 2002 WC₁₉ follow the trend of the higher-mass objects in both panels.

encounters with objects from the primordial Kuiper belt ejected by the giant planets into crossing the cold classical region. Since the disruption depends not on mass but on the a/R_H ratio (Parker and Kavelaars, 2010), it would be expected that low-mass and high-mass objects alike would

be similarly affected, and a population of wider binaries should also be seen among the higher-mass objects.

A solution to this problem could rest on the pebble accretion process. The small objects are planetesimals, too low-mass to undergo pebble accretion. In contrast, the higher

mass objects started as planetesimals at a closer distance to the Sun than they are now, and underwent significant growth by pebble accretion. Starting from a uniform distribution of a/R_H vs mass, pebble accretion might have disrupted by dynamical friction the original binaries of the now high-mass objects. This scenario would support the present model in which the current satellites of the high-mass Kuiper belt objects are the result of collisions (Canup, 2005; Brown et al., 2006; Canup, 2011; Brown and Butler, 2018; Arakawa et al., 2019; Bernstein et al., 2023; Brown and Butler, 2023). To date, no study of dynamical friction due to pebble accretion on the orbits of binaries has been undertaken.

Other effects could also result from non-Keplerian motion. We show in the lower panel of Fig. 3 the square of the ratio of primary radius to semi-major axis of the secondary, $(R_p/a)^2$, which we take as proxy for non-Keplerian motion, as this is the distance dilution factor for the quadrupole. The data on R_p was also taken from J19. As with the upper plot, in addition to the error bars, whiskers mark how the excursion in eccentricity from apoastron to periastron affects $(R_p/a)^2$. The dashed line shows the linear regression for the high-mass binaries. A trend is suggested, of larger quadrupole influence as the mass decreases. Inside the mass gap, the $(R_p/a)^2$ factor would range from about 5×10^{-3} to a little under 10^{-2} . Non-Keplerian effects do not necessarily lead to binary disruption, but they do complicate mass determinations, so it is possible that more binaries in the gap may have been detected but we simply do not know their masses yet.

The other possibility, of observational bias, is that binaries in the gap exist, with either a large companion that is nevertheless too close to the primary to discern a separation, or with a small satellite that is too dim to see. The worst case would of course be a satellite that is both too close to the primary and too dim. Given that the Hill radius is a slower function of mass than magnitude ($m^{1/3}$ vs $m^{2/3}$, respectively, where m is mass), a decrease in mass will thus be more pronounced in magnitude than in separation. Therefore, the hypothesis that the satellites exist but are too dim to observe may be the correct one.

As for the objects in the gap, Huya and 2002 WC₁₉, we pose the question: are they more similar to the low-mass objects, or to the high-mass objects? Given Fig. 1a, these objects do not follow the density trend of $\approx 0.5 \text{ g cm}^{-3}$ for low-mass objects, and increasing slightly due to gravitational pressure (Bierson and Nimmo, 2019) and/or silicate pebble accretion (Cañas et al., 2024). Huya has higher density ($1.073 \pm 0.066 \text{ g cm}^{-3}$) than 2002 UX₂₅ ($0.82 \pm 0.11 \text{ g cm}^{-3}$), an object about 3 times its mass. 2002 WC₁₉ is a more serious outlier, at an unphysical high density of $3.5 \pm 1.7 \text{ g cm}^{-3}$, similar to fully compact silicates (albeit with a high uncertainty). Determining radius from the thermal radiometry technique is not without issues. A lower albedo could get the density under 2 g cm^{-3} , but an unlikely low albedo would be needed to bring it to the $\lesssim 1 \text{ g cm}^{-3}$ values of the density trend (the same issue applies to Borasisi, which, at $2.1_{-1.2}^{+2.6} \text{ g cm}^{-3}$, also looks to be high density

compared to its cold classical cohort). On the other hand, as Fig. 3 shows, Huya and 2002 WC₁₉ follow very well the trend suggested by the high-mass objects, both for the anti-correlation of mass vs $(R_p/a)^2$, and the flat a/R_H . These characteristics suggest that Huya and 2002 WC₁₉ could be fragments of differentiated parent bodies or, if primordial, formed early enough to undergo melting and porosity removal from radiogenic heating.

We note that the gap in magnitude (Fig. 2), although less clear than the mass gap, is consistent with a bimodal distribution. The objects inside the $4 < H < 5$ gap are Salacia ($H = 4.24 \pm 0.02$), a scattered disk object on the high-mass side of the mass gap, and 2000 YW134 ($H = 4.72 \pm 0.03$), an object in 8:3 resonance with Neptune. Curiously, Salacia is dimmer than 3 objects with lower mass: 2002 UX₂₅ ($H = 3.88 \pm 0.01$), Varda (3.81 ± 0.01), and G!kúnll'hòmdímà ($H = 3.45 \pm 0.03$). As for 2000 YW134, it does not seem to have a dynamical mass determination. Yet, the orbital period estimate of the satellite, 10 days, coupled with a separation of $\approx 1900 \text{ km}$ (Stephens and Noll, 2006), implies a mass around $5 \times 10^{18} \text{ kg}$, and thus on the low-mass side of the mass gap, and the actual mass is probably even smaller (W. Grundy, private communication). We note that Huya ($H = 5.31 \pm 0.2$) and 2002 WC₁₉ ($H = 5.0 \pm 0.5$), although inside the mass gap, are on the dim side of the magnitude gap. This is expected given their smaller radii.

Other interesting cases are Vanth and Dysnomia, the satellites of Orcus and Eris, respectively. These are thought to have formed in collision events with undifferentiated bodies where the impactor is left “intact”, similar to the event that produced the Pluto-Charon system (Canup, 2005, 2011; Arakawa et al., 2019). Unlike collision events where mass from a differentiated body is cast into orbit, forming a predominantly icy object of high albedo (like the satellites of Haumea), in these events the satellite that remains is of roughly similar density as the impactor. Vanth has mass $(8.33 \pm 0.08) \times 10^{19} \text{ kg}$ (Brown and Butler, 2023), putting it in the gap, and density $1.5_{-0.5}^{+1.0} \text{ g cm}^{-3}$. Dysnomia has only 1σ upper limits, $1.4 \times 10^{20} \text{ kg}$ for mass and 1.2 g cm^{-3} for density (Brown and Butler, 2023), which would make it similar to G!kúnll'hòmdímà, but more probably lower mass and thus likely in the gap. Vanth is in the magnitude gap, at $H = 4.88$; Dysnomia is dimmer, at $H = 5.6$. Yet, if the collision hypothesis is correct, their masses are not primordial, as simulations of the collision events show that the resulting satellite is about 3 times less massive than the impactor (Canup, 2005, 2011). Versions of Fig. 1 with Vanth and Dysnomia at their current and triple mass are shown in Appendix B. Whatever their primordial mass, these objects support the hypothesis that the gap is an observational bias. Since they are secondaries, not primaries, their detection and mass determination are relatively simpler tasks than if they were the primaries accompanied by much smaller satellites.

4. Conclusion

In this letter, we underscore a gap in binaries in the Kuiper belt in the mass range between $\approx 10^{19}$ - 10^{20} kg, with a corresponding dearth in binaries between 4th and 5th absolute magnitude H . The gap has appeared in graphs in the literature before, but focus has been put on density trends or size ratio and separation of the binaries. Many objects exist in the gap, evidenced by the fact that the H magnitude distribution is continuous. The origin of the gap is unclear, but evidence points to it being a combination of formation imprint and observational bias. The low-mass end of the gap is consistent with the truncation of cold classicals at 400 km diameter, thought to be primordial, resulting from formation by streaming instability, which does show an exponential tapering at the high-mass end of the initial mass function. Cold classicals binaries are usually of equal mass, making them easy to detect. As such, we do not expect future discoveries of binaries in the gap to be equal brightness as common among the cold classicals; indeed, the objects in the gap, Huya and 2002 WC₁₉, follow the trend of the higher-mass objects of small satellites in tight orbits. The system of Huya and its satellite is similar to Orcus-Vanth in size ratio, and 2002 WC₁₉ is about 4 times larger than its satellite. They are also tight binaries, with a/R_H 0.2% and 0.4%, respectively.

At the high-mass side of the gap, the objects have small satellites, which poses an observational challenge as at low mass these small satellites would have to be too close to the primary to have survived interaction with either Neptune or the primordial belt, and possibly also too dim to detect with current observational capabilities. Mass determinations of objects in the gap may also be plagued by non-Keplerian effects given the trend of increasing $(R_p/a)^2$ with decreasing mass. We end this study then with the question: do smaller non-cold classicals objects have satellites? In a future study we will constrain the observational parameter space, in terms of magnitude and separation, that would be needed to discover these missing binaries, if they exist.

Acknowledgements

I acknowledge discussions with Mike Brown, Casey Lisse, Marc Buie, Daniel Carrera, and Will Grundy. The mass gap was first pointed out to me by Kaitlin Kratter, as a question following a talk where I showed Fig. 1 of Cañas et al. (2024). I thank the two anonymous referees for comments that helped improve the manuscript. This research was made possible by the NASA Emerging Worlds program, via grant No. 80NSSC22K1419.

Appendix

A. System mass vs primary mass

Given the ambiguity on using system mass, or primary mass (which needs information on radius ratio and assumption of equal density), we show here as supplementary

information a version of Fig. 1 with system mass (Fig. 4, panels a and b). We also show an analysis where primary mass was used only for the cold classicals and system mass for the other objects (Fig. 4, panels c and d), motivated by the fact that equal density is a safe assumption for the cold classicals only, as their equal colors evidence a common origin. For these cases, satellites (Triton and Charon) are removed, and Charon's mass is added to Pluto's. Conclusions are unchanged provided that, when using system mass, we change the bin interval and range from decimals numbers (10^{19} - 10^{20} kg) to between the masses of Lempo and 2002 UX₂₅.

B. Satellites

Given recent mass and radius determination of Vanth and an upper limit for Dysnomia (Brown and Butler, 2023) we show in Fig. 5, panels a and b, a version of Fig. 1 including them. Their masses fall in the gap; Vanth does not follow the density trend (having similar density to Orcus), whereas Dysnomia does, within the upper part of the uncertainty range. Fig. 5 panels c and d, are the same as a and b but for three times the mass of Charon, Dysnomia, and Vanth, considering the typical outcomes of the mass ratio of impactor to resulting satellite in the “intact fragment” collision model (Canup, 2005, 2011). Triton retains its mass since it was likely captured via 3-body interaction (Agnor and Hamilton, 2006), instead of a giant impact. With these modified masses, proto-Charon continues following the density trend, proto-Vanth now follows it, and proto-Dysnomia does not. If they are indeed intact fragments from an undifferentiated impactor, their densities being similar to the impactor, then this would imply that Vanth lost significant mass, whereas Dysnomia lost little. Such conclusion is highly uncertain, though, since Dysnomia seems to be in a regime intermediate between intact fragment and disk reaccretion (Arakawa et al., 2019).

References

- Agnor, C.B., Hamilton, D.P., 2006. Neptune’s capture of its moon Triton in a binary-planet gravitational encounter. *Nature* 441, 192–194. doi:10.1038/nature04792.
- Arakawa, S., Hyodo, R., Genda, H., 2019. Early formation of moons around large trans-Neptunian objects via giant impacts. *Nature Astronomy* 3, 802–807. doi:10.1038/s41550-019-0797-9, arXiv:1906.10833.
- Barucci, M.A., Boehnhardt, H., Cruikshank, D.P., Morbidelli, A., Dotson, R., 2008. The Solar System Beyond Neptune.
- Batygin, K., Brown, M.E., Fraser, W.C., 2011. Retention of a Primordial Cold Classical Kuiper Belt in an Instability-Driven Model of Solar System Formation. *ApJ* 738, 13. doi:10.1088/0004-637X/738/1/13, arXiv:1106.0937.
- Bernstein, G.M., Holler, B.J., Navarro-Escamilla, R., Bernardinelli, P.H., Abbott, T.M.C., Aguena, M., Allam, S., Alves, O., Andrade-Oliveira, F., Annis, J., Bacon, D., Brooks, D., Burke, D.L., Carnero Rosell, A., Carretero, J., da Costa, L.N., Pereira, M.E.S., De Vicente, J., Desai, S., Doel, P., Drlica-Wagner, A., Everett, S., Ferrero, I., Frieman, J., García-Bellido, J., Gerdes, D.W., Gruen, D., Gutierrez, G., Herner, K., Hinton, S.R., Hollowood, D.L., Honscheid, K., James, D.J., Kuehn, K., Kuropatkin, N., Marshall, J.L., Mena-Fernández, J., Miquel, R., Ogando, R.L.C., Pieres, A., Plazas Malagón, A.A., Raveri, M., Reil, K.,

Kuiper belt mass gap

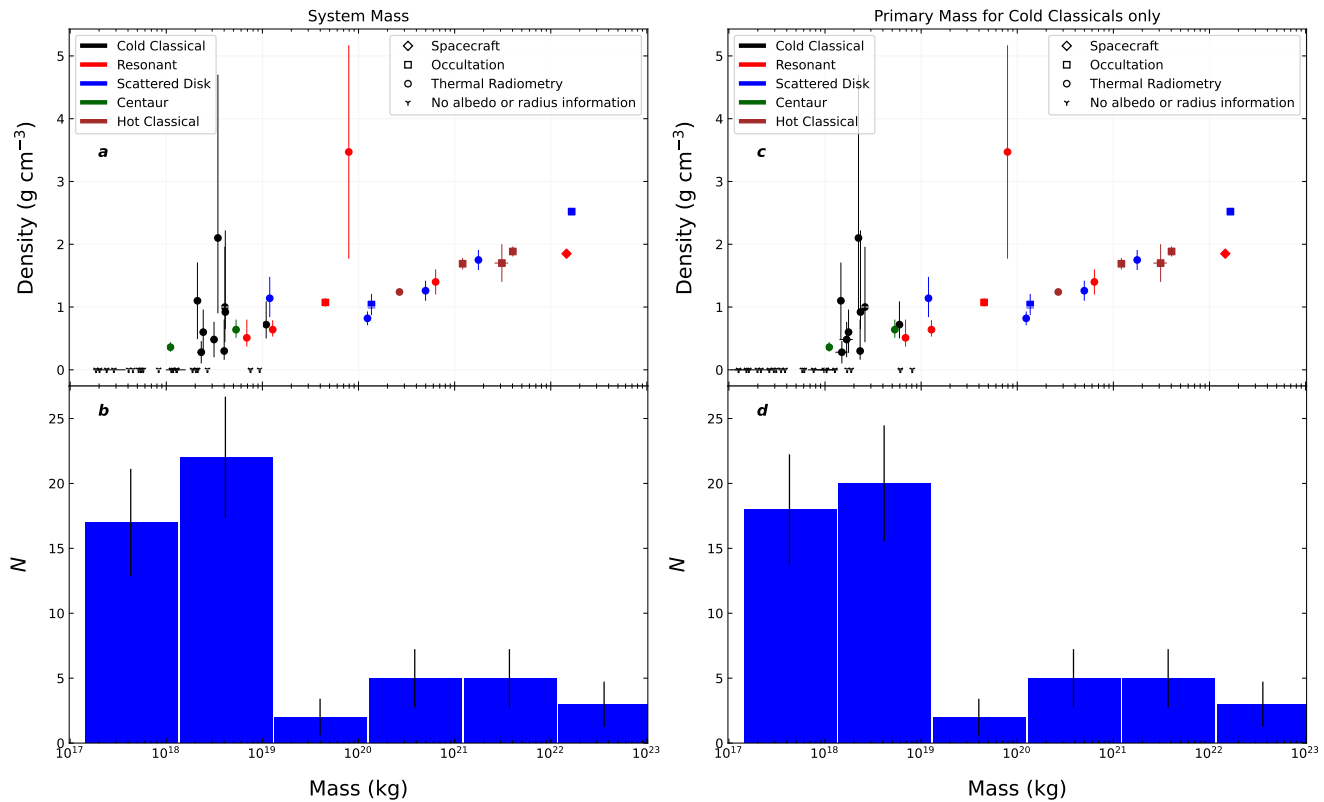


Figure 4: a and b) Same as Fig 1a and Fig 1b but for system mass. The bin size is the mass interval between Lempo and 2002 UX₂₅. c and d) Same as a and b but for primary mass only for the cold classicals. Satellites are excluded.

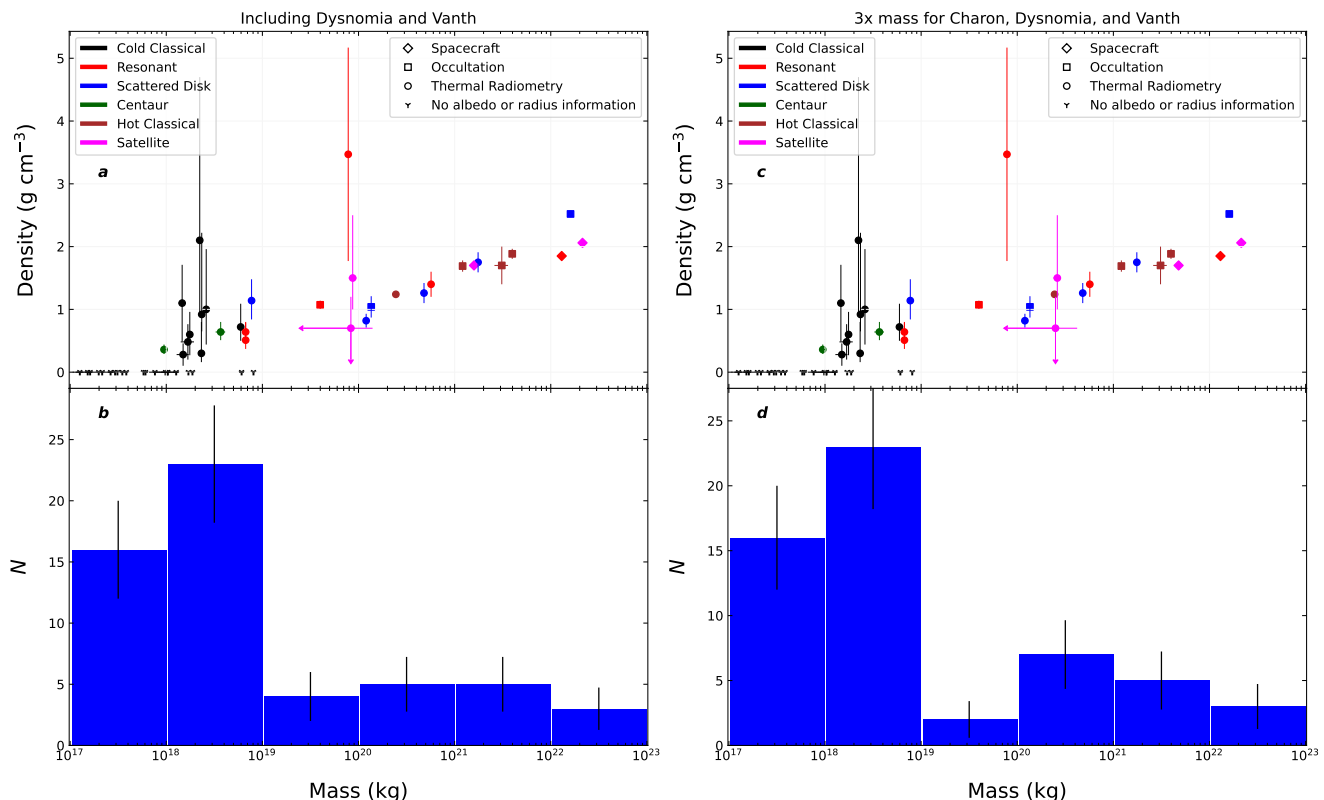


Figure 5: a and b) Same as Fig 1a and Fig 1b but including Vanth and Dysnomia. c and d) Same as a and b but tripling the mass of Charon, Vanth, and Dysnomia.

- Sanchez, E., Sevilla-Noarbe, I., Smith, M., Soares-Santos, M., Suchyna, E., Swanson, M.E.C., Wiseman, P., DES Collaboration, 2023. Synchronous Rotation in the (136199) Eris-Dysnomia System. *PSJ* 4, 115. doi:10.3847/PSJ/acdd5f, arXiv:2303.13445.
- Bernstein, G.M., Trilling, D.E., Allen, R.L., Brown, M.E., Holman, M., Malhotra, R., 2004. The Size Distribution of Trans-Neptunian Bodies. *AJ* 128, 1364–1390. doi:10.1086/422919, arXiv:astro-ph/0308467.
- Bierson, C.J., Nimmo, F., 2019. Using the density of Kuiper Belt Objects to constrain their composition and formation history. *Icarus* 326, 10–17. doi:10.1016/j.icarus.2019.01.027.
- Bottke, W.F., Vokrouhlický, D., Marschall, R., Nesvorný, D., Morbidelli, A., Deienno, R., Marchi, S., Dones, L., Levison, H.F., 2023. The Collisional Evolution of the Primordial Kuiper Belt, Its Destabilized Population, and the Trojan Asteroids. *PSJ* 4, 168. doi:10.3847/PSJ/ace7cd, arXiv:2307.07089.
- Braga-Ribas, F., Sicardy, B., Ortiz, J.L., Lellouch, E., Tancredi, G., Lecacheux, J., Vieira-Martins, R., Camargo, J.I.B., Assafin, M., Behrend, R., Vachier, F., Colas, F., Morales, N., Maury, A., Emilio, M., Amorim, A., Unda-Sanzana, E., Roland, S., Bruzzone, S., Almeida, L.A., Rodrigues, C.V., Jacques, C., Gil-Hutton, R., Vanzi, L., Milone, A.C., Schoenell, W., Salvo, R., Almenares, L., Jehin, E., Manfroid, J., Sposetti, S., Tanga, P., Klotz, A., Frappa, E., Cacella, P., Colque, J.P., Neves, C., Alvarez, E.M., Gillon, M., Pimentel, E., Giacchini, B., Roques, F., Widemann, T., Magalhães, V.S., Thirouin, A., Duffard, R., Leiva, R., Toledo, I., Capeche, J., Beisker, W., Pollock, J., Cedeño Montaña, C.E., Ivarsen, K., Reichart, D., Haislip, J., Lacluyze, A., 2013. The Size, Shape, Albedo, Density, and Atmospheric Limit of Transneptunian Object (50000) Quaoar from Multi-chord Stellar Occultations. *ApJ* 773, 26. doi:10.1088/0004-637X/773/1/26.
- Brown, M.E., 2013a. On the Size, Shape, and Density of Dwarf Planet Makemake. *ApJL* 767, L7. doi:10.1088/2041-8205/767/1/L7, arXiv:1304.1041.
- Brown, M.E., 2013b. The Density of Mid-sized Kuiper Belt Object 2002 UX25 and the Formation of the Dwarf Planets. *ApJL* 778, L34. doi:10.1088/2041-8205/778/2/L34, arXiv:1311.0553.
- Brown, M.E., Butler, B.J., 2017. The Density of Mid-sized Kuiper Belt Objects from ALMA Thermal Observations. *AJ* 154, 19. doi:10.3847/1538-3881/aa6346, arXiv:1702.07414.
- Brown, M.E., Butler, B.J., 2018. Medium-sized Satellites of Large Kuiper Belt Objects. *AJ* 156, 164. doi:10.3847/1538-3881/aad9f2, arXiv:1801.07221.
- Brown, M.E., Butler, B.J., 2023. Masses and Densities of Dwarf Planet Satellites Measured with ALMA. *PSJ* 4, 193. doi:10.3847/PSJ/ace52a, arXiv:2307.04848.
- Brown, M.E., van Dam, M.A., Bouchez, A.H., Le Mignant, D., Campbell, R.D., Chin, J.C.Y., Conrad, A., Hartman, S.K., Johansson, E.M., Lafon, R.E., Robinowitz, D.L., Stomski, Jr., P.J., Summers, D.M., Trujillo, C.A., Wizinowich, P.L., 2006. Satellites of the Largest Kuiper Belt Objects. *ApJL* 639, L43–L46. doi:10.1086/501524, arXiv:astro-ph/0510029.
- Brozović, M., Jacobson, R.A., 2024. Post-new-horizons Orbits and Masses for the Satellites of Pluto. *AJ* 167, 256. doi:10.3847/1538-3881/ad39f0.
- Brunini, A., Zanardi, M., 2016. Dynamical and collisional evolution of Kuiper belt binaries. *MNRAS* 455, 4487–4497. doi:10.1093/mnras/stv2602.
- Cañas, M.H., Lyra, W., Carrera, D., Krapp, L., Sengupta, D., Simon, J.B., Umurhan, O.M., Yang, C.C., Youdin, A.N., 2024. A Solution for the Density Dichotomy Problem of Kuiper Belt Objects with Multispecies Streaming Instability and Pebble Accretion. *PSJ* 5, 55. doi:10.3847/PSJ/ad1d5b, arXiv:2401.04294.
- Campbell, H.M., Anderson, K.E., Kaib, N.A., 2025. A non-primordial origin for the widest binaries in the Kuiper belt. *Nature Astronomy* 9, 75–80. doi:10.1038/s41550-024-02388-4, arXiv:2411.09908.
- Campbell, H.M., Stone, L.R., Kaib, N.A., 2023. Close Trans-Neptunian Object Passages as a Driver of the Origin and Evolution of Ultrawide Kuiper Belt Binaries. *AJ* 165, 19. doi:10.3847/1538-3881/aca08e, arXiv:2211.06383.
- Canup, R.M., 2005. A Giant Impact Origin of Pluto-Charon. *Science* 307, 546–550. doi:10.1126/science.1106818.
- Canup, R.M., 2011. On a Giant Impact Origin of Charon, Nix, and Hydra. *AJ* 141, 35. doi:10.1088/0004-6256/141/2/35.
- Christy, J.W., Harrington, R.S., 1978. The satellite of Pluto. *AJ* 83, 1005. doi:10.1086/112284.
- Descamps, P., 2015. Dumb-bell-shaped equilibrium figures for fiducial contact-binary asteroids and EKBOs. *Icarus* 245, 64–79. doi:10.1016/j.icarus.2014.08.002, arXiv:1410.7962.
- Dones, L., Brasser, R., Kaib, N., Rickman, H., 2015. Origin and Evolution of the Cometary Reservoirs. *SSR* 197, 191–269. doi:10.1007/s11214-015-0223-2.
- Fraser, W.C., Brown, M.E., Schwamb, M.E., 2010. The luminosity function of the hot and cold Kuiper belt populations. *Icarus* 210, 944–955. doi:10.1016/j.icarus.2010.08.001, arXiv:1008.1058.
- Gomes, R., Levison, H.F., Tsiganis, K., Morbidelli, A., 2005. Origin of the cataclysmic Late Heavy Bombardment period of the terrestrial planets. *Nature* 435, 466–469. doi:10.1038/nature03676.
- Grundy, W.M., Noll, K.S., Roe, H.G., Buie, M.W., Porter, S.B., Parker, A.H., Nesvorný, D., Levison, H.F., Benecchi, S.D., Stephens, D.C., Trujillo, C.A., 2019. Mutual orbit orientations of transneptunian binaries. *Icarus* 334, 62–78. doi:10.1016/j.icarus.2019.03.035.
- Grundy, W.M., Porter, S.B., Benecchi, S.D., Roe, H.G., Noll, K.S., Trujillo, C.A., Thirouin, A., Stansberry, J.A., Barker, E., Levison, H.F., 2015. The mutual orbit, mass, and density of the large transneptunian binary system Varda and Ilmarë. *Icarus* 257, 130–138. doi:10.1016/j.icarus.2015.04.036, arXiv:1505.00510.
- Hahn, J.M., 2003. The Secular Evolution of the Primordial Kuiper Belt. *ApJ* 595, 531–549. doi:10.1086/377195, arXiv:astro-ph/0305602.
- Jewitt, D., Luu, J., 1993. Discovery of the candidate Kuiper belt object 1992 QB₁. *Nature* 362, 730–732. doi:10.1038/362730a0.
- Johansen, A., Mac Low, M.M., Lacerda, P., Bizzarro, M., 2015. Growth of asteroids, planetary embryos, and Kuiper belt objects by chondrule accretion. *Science Advances* 1, 1500109. doi:10.1126/sciadv.1500109, arXiv:1503.07347.
- Johnston, W.R., 2019. Binary Minor Planets Compilation V3.0. NASA Planetary Data System, urn:nasa:pds:ast_binary_parameters_compilation::3.0. doi:10.26033/bb68-pw96.
- Kavelaars, J.J., Petit, J.M., Gladman, B., Bannister, M.T., Alexandersen, M., Chen, Y.T., Gwyn, S.D.J., Volk, K., 2021. OSSOS Finds an Exponential Cutoff in the Size Distribution of the Cold Classical Kuiper Belt. *ApJL* 920, L28. doi:10.3847/2041-8213/ac2c72, arXiv:2107.06120.
- Kiss, C., Marton, G., Parker, A.H., Grundy, W.M., Farkas-Takács, A., Stansberry, J., Pál, A., Müller, T., Noll, K.S., Schwamb, M.E., Barr, A.C., Young, L.A., Vinkó, J., 2019. The mass and density of the dwarf planet (225088) 2007 OR₁₀. *Icarus* 334, 3–10. doi:10.1016/j.icarus.2019.03.013, arXiv:1903.05439.
- Kovalenko, I.D., Doressoundiram, A., Lellouch, E., Vilenius, E., Müller, T., Stansberry, J., 2017. “TNOs are Cool”: A survey of the trans-Neptunian region. XIII. Statistical analysis of multiple trans-Neptunian objects observed with Herschel Space Observatory. *A&A* 608, A19. doi:10.1051/0004-6361/201730588.
- Lacerda, P., 2011. A Change in the Light Curve of Kuiper Belt Contact Binary (139775) 2001 QG₂₉₈. *AJ* 142, 90. doi:10.1088/0004-6256/142/3/90, arXiv:1107.3507.
- Lellouch, E., Santos-Sanz, P., Lacerda, P., Mommert, M., Duffard, R., Ortiz, J.L., Müller, T.G., Fornasier, S., Stansberry, J., Kiss, C., Vilenius, E., Mueller, M., Peixinho, N., Moreno, R., Grousson, O., Delsanti, A., Harris, A.W., 2013. “TNOs are Cool”: A survey of the trans-Neptunian region. IX. Thermal properties of Kuiper belt objects and Centaurs from combined Herschel and Spitzer observations. *A&A* 557, A60. doi:10.1051/0004-6361/20132047.
- Lyra, W., Johansen, A., Cañas, M.H., Yang, C.C., 2023. An Analytical Theory for the Growth from Planetesimals to Planets by Polydisperse Pebble Accretion. *arXiv e-prints*, arXiv:2301.03825doi:10.48550/arXiv.2301.03825, arXiv:2301.03825.
- Malhotra, R., 2019. Resonant Kuiper belt objects: a review. *Geoscience Letters* 6, 12. doi:10.1186/s40562-019-0142-2, arXiv:1911.07897.
- McKinnon, W.B., Stern, S.A., Weaver, H.A., Nimmo, F., Bierson, C.J.,

- Grundy, W.M., Cook, J.C., Cruikshank, D.P., Parker, A.H., Moore, J.M., Spencer, J.R., Young, L.A., Olkin, C.B., Ennico Smith, K., New Horizons Geology, G., Imaging, Composition Theme Teams, 2017. Origin of the Pluto-Charon system: Constraints from the New Horizons flyby. *Icarus* 287, 2–11. doi:[10.1016/j.icarus.2016.11.019](https://doi.org/10.1016/j.icarus.2016.11.019).
- Morbidelli, A., Brown, M.E., Morbidelli, H.F., 2003. The Kuiper Belt and its Primordial Sculpting. *Earth Moon and Planets* 92, 1–27. doi:[10.1023/B:MOON.0000031921.37380.80](https://doi.org/10.1023/B:MOON.0000031921.37380.80).
- Morbidelli, A., Levison, H.F., Gomes, R., 2008. The Dynamical Structure of the Kuiper Belt and Its Primordial Origin, in: Barucci, M.A., Boehnhardt, H., Cruikshank, D.P., Morbidelli, A., Dotson, R. (Eds.), *The Solar System Beyond Neptune*, pp. 275–292. doi:[10.48550/arXiv.astro-ph/0703558](https://doi.org/10.48550/arXiv.astro-ph/0703558).
- Morbidelli, A., Nesvorný, D., 2020. Kuiper belt: formation and evolution, in: Prialnik, D., Barucci, M.A., Young, L. (Eds.), *The Trans-Neptunian Solar System*, pp. 25–59. doi:[10.1016/B978-0-12-816490-7.00002-3](https://doi.org/10.1016/B978-0-12-816490-7.00002-3).
- Morbidelli, A., Valsecchi, G.B., 1997. NOTE: Neptune Scattered Planesimals Could Have Sculpted the Primordial Edgeworth-Kuiper Belt. *Icarus* 128, 464–468. doi:[10.1006/icar.1997.5745](https://doi.org/10.1006/icar.1997.5745).
- Morgado, B.E., Sicardy, B., Braga-Ribas, F., Ortiz, J.L., Salo, H., Vachier, F., Desmars, J., Pereira, C.L., Santos-Sanz, P., Sfair, R., de Santana, T., Assafin, M., Vieira-Martins, R., Gomes-Júnior, A.R., Margot, G., Dhillon, V.S., Fernández-Valenzuela, E., Broughton, J., Bradshaw, J., Langsek, R., Benedetti-Rossi, G., Souami, D., Holler, B.J., Kretlow, M., Boufleur, R.C., Camargo, J.I.B., Duffard, R., Beisker, W., Morales, N., Lecacheux, J., Rommel, F.L., Herald, D., Benz, W., Jehin, E., Jankowsky, F., Marsh, T.R., Littlefair, S.P., Bruno, G., Pagano, I., Brandeker, A., Collier-Cameron, A., Florén, H.G., Hara, N., Olofsson, G., Wilson, T.G., Benkhaldoun, Z., Busutil, R., Burdanov, A., Ferrais, M., Gault, D., Gillon, M., Hanna, W., Kerr, S., Kolb, U., Nosworthy, P., Sebastian, D., Snodgrass, C., Teng, J.P., de Wit, J., 2023. A dense ring of the trans-Neptunian object Quaoar outside its Roche limit. *Nature* 614, 239–243. doi:[10.1038/s41586-022-05629-6](https://doi.org/10.1038/s41586-022-05629-6).
- Müller, T.G., Lellouch, E., Stansberry, J., Kiss, C., Santos-Sanz, P., Vilenius, E., Protopapa, S., Moreno, R., Mueller, M., Delsanti, A., Duffard, R., Fornasier, S., Groussin, O., Harris, A.W., Henry, F., Horner, J., Lacerda, P., Lim, T., Mommert, M., Ortiz, J.L., Rengel, M., Thirouin, A., Trilling, D., Barucci, A., Crovisier, J., Doressoundiram, A., Dotto, E., Gutiérrez, P.J., Hainaut, O.R., Hartogh, P., Hestroffer, D., Kidger, M., Lara, L., Swinyard, B., Thomas, N., 2010. “TNOs are Cool”: A survey of the trans-Neptunian region. I. Results from the Herschel science demonstration phase (SDP). *A&A* 518, L146. doi:[10.1051/0004-6361/201014683](https://doi.org/10.1051/0004-6361/201014683), arXiv:1005.2923.
- Noll, K., Grundy, W.M., Nesvorný, D., Thirouin, A., 2020. Trans-Neptunian binaries (2018), in: Prialnik, D., Barucci, M.A., Young, L. (Eds.), *The Trans-Neptunian Solar System*, pp. 201–224. doi:[10.1016/B978-0-12-816490-7.00009-6](https://doi.org/10.1016/B978-0-12-816490-7.00009-6).
- Noll, K.S., Grundy, W.M., Chiang, E.I., Margot, J.L., Kern, S.D., 2008a. Binaries in the Kuiper Belt. p. 345.
- Noll, K.S., Grundy, W.M., Stephens, D.C., Levison, H.F., Kern, S.D., 2008b. Evidence for two populations of classical transneptunian objects: The strong inclination dependence of classical binaries. *Icarus* 194, 758–768. doi:[10.1016/j.icarus.2007.10.022](https://doi.org/10.1016/j.icarus.2007.10.022), arXiv:0711.1545.
- Parker, A.H., Kavelaars, J.J., 2010. Destruction of Binary Minor Planets During Neptune Scattering. *ApJL* 722, L204–L208. doi:[10.1088/2041-8205/722/2/L204](https://doi.org/10.1088/2041-8205/722/2/L204), arXiv:1009.3495.
- Parker, A.H., Kavelaars, J.J., Petit, J.M., Jones, L., Gladman, B., Parker, J., 2011. Characterization of Seven Ultra-wide Trans-Neptunian Binaries. *ApJ* 743, 1. doi:[10.1088/0004-637X/743/1/1](https://doi.org/10.1088/0004-637X/743/1/1), arXiv:1108.2505.
- Pereira, C.L., Sicardy, B., Morgado, B.E., Braga-Ribas, F., Fernández-Valenzuela, E., Souami, D., Holler, B.J., Boufleur, R.C., Margot, G., Assafin, M., Ortiz, J.L., Santos-Sanz, P., Epinat, B., Kervella, P., Desmars, J., Vieira-Martins, R., Kilic, Y., Gomes Júnior, A.R., Camargo, J.I.B., Emilio, M., Vara-Lubiano, M., Kretlow, M., Albert, L., Alcock, C., Ball, J.G., Bender, K., Buie, M.W., Butterfield, K., Camarca, M., Castro-Chacón, J.H., Dunford, R., Fisher, R.S., Gamble, D., Geary, J.C., Gnilka, C.L., Green, K.D., Hartman, Z.D., Huang, C.K., Januszewski, H., Johnston, J., Kagitani, M., Kamin, R., Kavelaars, J.J., Keller, J.M., de Kleer, K.R., Lehner, M.J., Luken, A., Marchis, F., Marlin, T., McGregor, K., Nikitin, V., Nothenius, R., Patrick, C., Redfield, S., Rengstorf, A.W., Reyes-Ruiz, M., Seccull, T., Skrutskie, M.F., Smith, A.B., Sproul, M., Stephens, A.W., Szentgyorgyi, A., Sánchez-Sanjuán, S., Tatsumi, E., Verbiscer, A., Wang, S.Y., Yoshida, F., Young, R., Zhang, Z.W., 2023. The two rings of (50000) Quaoar. *A&A* 673, L4. doi:[10.1051/0004-6361/202346365](https://doi.org/10.1051/0004-6361/202346365), arXiv:2304.09237.
- Petit, J.M., Kavelaars, J.J., Gladman, B.J., Jones, R.L., Parker, J.W., Van Laerhoven, C., Nicholson, P., Mars, G., Rousselot, P., Mousis, O., Marsden, B., Bieryla, A., Taylor, M., Ashby, M.L.N., Benavidez, P., Campo Bagatin, A., Bernabeu, G., 2011. The Canada-France Ecliptic Plane Survey—Full Data Release: The Orbital Structure of the Kuiper Belt. *AJ* 142, 131. doi:[10.1088/0004-6256/142/4/131](https://doi.org/10.1088/0004-6256/142/4/131), arXiv:1108.4836.
- Petit, J.M., Kavelaars, J.J., Gladman, B.J., Margot, J.L., Nicholson, P.D., Jones, R.L., Parker, J.W., Ashby, M.L.N., Campo Bagatin, A., Benavidez, P., Coffey, J., Rousselot, P., Mousis, O., Taylor, P.A., 2008. The Extreme Kuiper Belt Binary 2001 QW₃₂₂. *Science* 322, 432. doi:[10.1126/science.1163148](https://doi.org/10.1126/science.1163148).
- Prialnik, D., Barucci, M.A., Young, L., 2020. The Trans-Neptunian Solar System.
- Proudfoot, B.C.N., Ragazzine, D.A., Thatcher, M.L., Grundy, W., Spencer, D.J., Alailima, T.M., Allen, S., Bowden, P.C., Byrd, S., Camacho, C.D., Campbell, G.H., Carlisle, E.P., Christensen, J.A., Christensen, N.K., Clement, K., Derieg, B.J., Dille, M.K., Dorrett, C., Ellefson, A.L., Fleming, T.S., Freeman, N.J., Gibson, E.J., Giforos, W.G., Guerrette, J.A., Haddock, O., Hammond, S.A., Hampson, Z.A., Hancock, J.D., Harmer, M.S., Henderson, J.R., Jensen, C.R., Jensen, D., Jensen, R.E., Jones, J.S., Kubal, C.C., Lunt, J.N., Martins, S., Matheson, M., Maxwell, D., Morrell, T.D., Myckowiak, M.M., Nelsen, M.A., Neu, S.T., Nuccitelli, G.G., Reardon, K.M., Reid, A.S., Richards, K.G., Robertson, M.R.W., Rydalch, T.D., Scoresby, C.B., Scott, R.L., Shakespear, Z.D., Silveira, E.A., Steed, G.C., Suggs, C.Z., Suggs, G.D., Tobias, D.M., Toole, M.L., Townsend, M.L., Vickers, K.L., Wagner, C.R., Wright, M.S., Zappala, E.M.A., 2024. Beyond Point Masses. II. Non-Keplerian Shape Effects Are Detectable in Several TNO Binaries. *AJ* 167, 144. doi:[10.3847/1538-3881/ad26f0](https://doi.org/10.3847/1538-3881/ad26f0), arXiv:2403.12783.
- Rommel, F.L., Fernández-Valenzuela, E., Proudfoot, B.C.N., Ortiz, J.L., Morgado, B.E., Sicardy, B., Morales, N., Braga-Ribas, F., Desmars, J., Vieira-Martins, R., Holler, B.J., Kilic, Y., Grundy, W., Rizos, J.L., Camargo, J.I.B., Benedetti-Rossi, G., Gomes-Júnior, A., Assafin, M., Santos-Sanz, P., Kretlow, M., Vara-Lubiano, M., Leiva, R., Ragazzine, D.A., Duffard, R., Kučáková, H., Hornoch, K., Nikitin, V., Santana-Ros, T., Canales-Moreno, O., Lafuente-Aznar, D., Calavia-Belloc, S., Perelló, C., Selva, A., Organero, F., Hernandez, L.A., Cueva, I.d.l., Yuste-Moreno, M., García-Navarro, E., Donate-Lucas, J.E., Izquierdo-Carrión, L., Iglesias-Marzoa, R., Lacruz, E., Gonçalves, R., Staels, B., Goossens, R., Henden, A., Walker, G., Reyes, J.A., Pastor, S., Kaspi, S., Skrutskie, M., Verbiscer, A.J., Martinez, P., André, P., Maestre, J.L., Aceituno, F.J., Bacci, P., Maestripieri, M., Grazia, M.D., Castro-Tirado, A.J., Pérez-García, I., Fernández García, E.J., Fernández, E., Messner, S., Scarfi, G., Mikuž, H., Prat, J., Martorell, P., Nardiello, D., Nascimbeni, V., Sfair, R., Siqueira, P.B., Lattari, V., Liberato, L., Pinheiro, T.F.L.L., de Santana, T., Pereira, C.L., Alava-Amat, M.A., Ciabattari, F., González-Rodríguez, H., Schnabel, C., 2025. Stellar Occultation Observations of (38628) Huya and Its Satellite: A Detailed Look into the System. *PSJ* 6, 48. doi:[10.3847/PSJ/adabc1](https://doi.org/10.3847/PSJ/adabc1), arXiv:2501.09739.
- Sheppard, S.S., Ragazzine, D., Trujillo, C., 2012. 2007 TY430: A Cold Classical Kuiper Belt Type Binary in the Plutino Population. *AJ* 143, 58. doi:[10.1088/0004-6256/143/3/58](https://doi.org/10.1088/0004-6256/143/3/58), arXiv:1112.2708.
- Sicardy, B., Bellucci, A., Gendron, E., Lacombe, F., Lacour, S., Lecacheux, J., Lellouch, E., Renner, S., Pau, S., Roques, F., Widemann, T., Colas, F., Vachier, F., Martins, R.V., Aogeorges, N., Hainaut, O., Marco, O., Beisker, W., Hummel, E., Feinstein, C., Levato, H., Maury, A., Frappa, E., Gaillard, B., Lavayssiére, M., di Sora, M., Mallia, F., Masi, G., Behrend, R., Carrier, F., Staelens, O., Rousselot, P., Alvarez-Candal, A., Lazzaro, D., Veiga, C., Andrei, A.H., Assafin, M., da Silva Neto, D.N., Jacques, C., Pimentel, E., Weaver, D., Lecampion, J.F., Doncel, F., Momiyama, T., Tancredi, G., 2006. Charon’s size and an upper

limit on its atmosphere from a stellar occultation. *Nature* 439, 52–54.

doi:10.1038/nature04351.

Slipher, V.M., 1930. Planet X-Lowell Observatory Observation Circular.

Journ. Royal Astron. Soc. of Canada 24, 282.

Stansberry, J., Grundy, W., Brown, M., Cruikshank, D., Spencer, J.,

Trilling, D., Margot, J.L., 2008. Physical Properties of Kuiper Belt and Centaur Objects: Constraints from the Spitzer Space Telescope, in: Barucci, M.A., Boehnhardt, H., Cruikshank, D.P., Morbidelli, A., Dotson, R. (Eds.), *The Solar System Beyond Neptune*, pp. 161–179. doi:10.48550/arXiv.astro-ph/0702538.

Stephens, D.C., Noll, K.S., 2006. Detection of Six Trans-Neptunian Binaries with NICMOS: A High Fraction of Binaries in the Cold Classical Disk. *AJ* 131, 1142–1148. doi:10.1086/498715, arXiv:astro-ph/0510130.

Stern, S.A., 1996. On the Collisional Environment, Accretion Time Scales, and Architecture of the Massive, Primordial Kuiper Belt. *AJ* 112, 1203. doi:10.1086/118091.

Stern, S.A., Colwell, J.E., 1997. Collisional Erosion in the Primordial Edgeworth-Kuiper Belt and the Generation of the 30–50 AU Kuiper Gap. *ApJ* 490, 879–882. doi:10.1086/304912.

Tombaugh, C.W., 1946. The Search for the Ninth Planet, Pluto. Leaflet of the Astronomical Society of the Pacific 5, 73.

Tsiganis, K., Gomes, R., Morbidelli, A., Levison, H.F., 2005. Origin of the orbital architecture of the giant planets of the Solar System. *Nature* 435, 459–461. doi:10.1038/nature03539.

Vilenius, E., Kiss, C., Müller, T., Mommert, M., Santos-Sanz, P., Pál, A., Stansberry, J., Mueller, M., Peixinho, N., Lellouch, E., Fornasier, S., Delsanti, A., Thirouin, A., Ortiz, J.L., Duffard, R., Perna, D., Henry, F., 2014. “TNOs are Cool”: A survey of the trans-Neptunian region. X. Analysis of classical Kuiper belt objects from Herschel and Spitzer observations. *A&A* 564, A35. doi:10.1051/0004-6361/201322416, arXiv:1403.6309.